Experimental and Kinetic Study on Ignition Delay Times of DME/n-Butane/O2/Ar Mixtures

6 AUTHORS, INCLUDING:

Erjiang Hu
Xi'an Jiaotong University
64 PUBLICATIONS **724** CITATIONS

SEE PROFILE

Zuohua Huang
Xi'an Jiaotong University
421 PUBLICATIONS **5,195** CITATIONS

SEE PROFILE

Shaodong Niu
51 PUBLICATIONS **253** CITATIONS

SEE PROFILE

Zhang Zihang
Xi'an Jiaotong University
21 PUBLICATIONS **56** CITATIONS

SEE PROFILE

Experimental and Kinetic Studies on Ignition Delay Times of Dimethyl Ether/*n*-Butane/O₂/Ar Mixtures

Erjiang Hu, Xue Jiang, Zuohua Huang,* Jiaxiang Zhang, Zihang Zhang, and Xingjia Man

State Key Laboratory of Multiphase Flow in Power Engineering, Xi'an Jiaotong University, Xi'an 710049, People's Republic of China

Ⓢ Supporting Information

ABSTRACT: Ignition delay times of stoichiometric dimethyl ether (DME) and *n*-butane blends were measured using shock tube at varied DME blending ratios (0, 30, 70, and 100%), temperatures (1200−1600 K), and pressures (1.2−5.3 atm). Simulation work was conducted using the Chemkin code with a NUI C4_47 mechanism. Correlations of ignition delay times were obtained on the basis of the measured data through multiple linear regressions. Results show that the ignition delay times increase linearly with the increase of $1000/T$, and this indicates that the overall activation energy is kept unchanged at the conditions in the study. Increasing pressure decreases the ignition delay time. Ignition delay time decreases with the increase of the DME blending ratio. The peak mole fractions of H and OH radicals increase, and the timing at the peak value of H and OH radicals advances as DME increases. Analysis on the reaction pathway shows that, at high temperatures, hydrogen-abstraction reactions play a dominant role in the consumption of fuel rather than the unimolecular decomposition reactions. At high temperatures, chemical reactions of two fuel components are independent. Sensitivity analysis shows that the dominant reactions affecting ignition delay time are the reactions that mainly involve the participation of small molecules.

1. INTRODUCTION

Homogenous charge compression ignition (HCCI) is a promising combustion mode in internal combustion engines. The in-cylinder temperature and pressure rise as compression proceeds and ignition simultaneously occurs over the multi-point of the combustible mixture without an obvious flame front. The lean homogeneous mixture and low-temperature combustion leads to low NO_x and particulate matter (PM), with high thermal efficiency, especially at low-load operation.

There are two approaches to achieve the HCCI combustion. One approach is by changing the fuel property (such as octane number and cetane number) using the blended fuels, and another approach is through changing engine operation and design parameters. Fuel blending is an efficient way of controlling HCCI combustion. Adjusting the fuel cetane number and/or octane number through fuel blending can meet various operation conditions of the HCCI combustion. Usually, blending of a high octane fuel and a high cetane fuel is used to adjust fuel property. Up to now, many fuel blends were tested in HCCI combustion, such as the *n*-heptane and iso-octane blend,[1] dimethyl ether (DME) and methane blend,[2,3] DME and liquefied petroleum gas (LPG) blend,[4] and DME and *n*-butane blend.[5,6]

In this study, the DME/*n*-butane blends are selected as the tested fuels. Engine combustion fueled with neat DME or DME/hydrocarbon (HC) blends has been reported in previous studies.[7−12,2−4] Ji et al.[7−10] investigated combustion and emissions of a spark-ignition (SI) engine fueled with DME blended with gasoline, methane, and ethane and found that DME blending could increase the indicated thermal efficiency and reduce HC emissions for SI engines. DME addition is an effective way for improving the performance of SI engines. Lu et al.[11,12] studied the HCCI combustion fueled with DME and demonstrated that ultralow NO_x emissions were realized

without smoke emission and NO_x emissions were also less than those of the direct-injection engine fueled with diesel. Sato et al.[2] studied the characteristics of HCCI combustion of the methane/DME/air mixture. The study indicated that DME becomes an ignition improver when blending with methane. Kong et al.[3] studied the natural gas/DME combustion in HCCI engines through computational fluid dynamics (CFD) simulation with detailed chemical kinetics. Their study showed that ignition could be improved by DME oxidation and low-temperature heat release is more pronounced as DME increases. Lee et al.[4] studied the effect of the blending of *n*-butane and propane on the performance and emissions of a SI engine fueled with DME-blended LPG fuel. Stable engine operation was achieved over a wide range of engine loads when fueled with the propane-containing LPG/DME fuels compared to the *n*-butane-containing LPG/DME fuels because of the high octane number of propane.

The previous studies showed that the study on the HCCI engine fueled with DME/HC blends mainly concentrated on the DME/methane blend, and there are limited reports on HCCI engine combustion fueled with the DME/*n*-butane blend. Iida et al.[5,6] studied the HCCI combustion character-istics fueled with the DME/*n*-butane blends in both an engine and a rapid compression machine at different blending ratios and exhaust gas recirculation (EGR) ratios, and they found that, by changing the blending ratio and EGR ratio, the HCCI combustion at different loads could be realized.

Fuel ignition delay time is an important parameter to control the HCCI ignition timing, and it is also the key parameter to develop and validate the chemical kinetics. The fuel−oxidizer
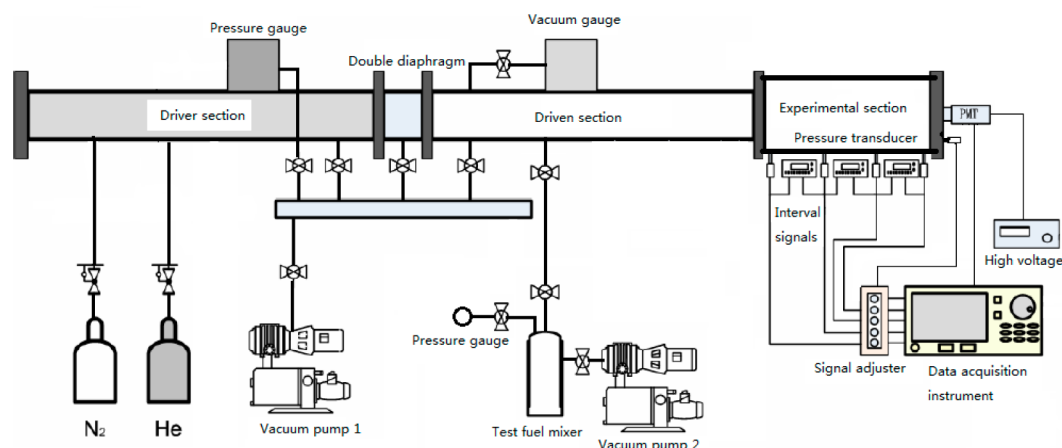
Figure 1. Schematic diagram of the shock tube.

mixtures are zero-dimensional and homogeneous in the shock tube, and they are ignited by the controlling of chemical kinetics. This is consistent with that in a HCCI combustion engine. Additionally, a shock tube can easily study the ignition delay time of fuel at a specified pressure and temperature, but a HCCI combustion engine cannot. Therefore, the measured ignition delay times in a shock tube are important to provide a guidance to a HCCI combustion engine.

The fundamental combustion and ignition characteristics of neat DME and DME/HC blends were extensively reported in the literature.[13−19] Pfahl et al.[13] studied the autoignition of DME/air in a shock tube at high pressure and low-to-intermediate temperatures. They found that DME had a two-step autoignition process at low temperatures, and a negative temperature coefficient (NTC) behavior was recognized. Mittal et al.[14] measured the ignition delay time of $DME/O_2/N_2$ mixtures at elevated pressures (10−20 bar) and low temperatures (615−735 K) in a rapid compression machine, and two-step self-ignition was also observed. This behavior becomes more prominent for the low-pressure and oxygen-lean mixtures. Dagaut et al.[15] and Cook et al.[16] measured the ignition delay times of DME in argon-diluted oxygen at high temperatures. They found that the Zhao mechanism[17] could predict the ignition delay times well. The study by Amano et al.[18] showed that DME could improve the ignition and combustion of methane−air mixtures both experimentally and numerically. Chen et al.[19] studied the effects of DME addition on the high-temperature ignition and combustion characteristics of methane−air mixtures. Their results showed that the addition of a small amount of DME into methane could result in a significant decrease in the ignition delay time at high temperatures. Up to now, the study on the ignition delay times of DME/HC blends mainly focused on the DME/methane blends and those of the DME/n-butane blends are not reported. Thus, the ignition delay times of the DME/n-butane are worth studying for both HCCI engine control and chemical kinetic development.

In this study, ignition delay times of DME/n-butane/O₂/Ar mixtures were measured in a shock tube at different pressures, temperatures, and DME blending ratios and an Arrhenius correlation is obtained through the multiple linear regression of the measured data. Furthermore, analysis on chemical kinetics was made using the Chemkin package. The reaction pathway and sensitivity analysis were made to provide insight on the ignition behavior when DME is added to n-butane.

2. EXPERIMENTAL SETUP AND NUMERICAL APPROACH

Ignition delay times were measured in a shock tube with an inner diameter of 11.5 cm, as shown in Figure 1. The shock tube is divided into a 4.0 m long driver section and a 4.8 m long driven section with double diaphragms. The pressures behind reflected shock waves are changed by applying different thickness polyester terephthalate (PET) films. High-purity helium (99.999%) is selected as the driver gas. The driven section is evacuated below 10^{-6} mbar by a vacuum system. Fuel mixtures are prepared in a 128 L cylindrical tank and introduced into the driver section after 12 h to ensure full homogeneity. Four sidewall pressure transducers (PCB 113B26) are located along the driven section with the same interval of 30 cm. The three time intervals are measured by three time counters (Fluke PM6690), with which the velocity of the shock wave at the endwall is determined by extrapolating the axial velocity profile to the endwall. A pressure transducer (PCB 113B03) is used to measure the pressure at the endwall. Endwall CH* emission is detected at 430 nm using a photomultiplier (Hamamatsu CR 131). All data acquisition is carried out by a digital recorder (Yokogama, DL750). The uncertainty of the temperature behind the reflected shock wave is less than 25 K. The detailed experimental setup and its validation have been mentioned previously in refs 20 and 21.

Ignition delay time (τ) is defined as the time interval between the time in which the incident shock wave arrived at the endwall and the intercept of the maximum slope of the CH* emission profile with the baseline, as shown in Figure 2.

Four stoichiometric fuel mixtures of DME/n-butane/O₂/Ar were tested in the study as shown in Table 1, where the argon/oxygen dilution ratio (D) is fixed at 15. Monatomic argon is often used as a
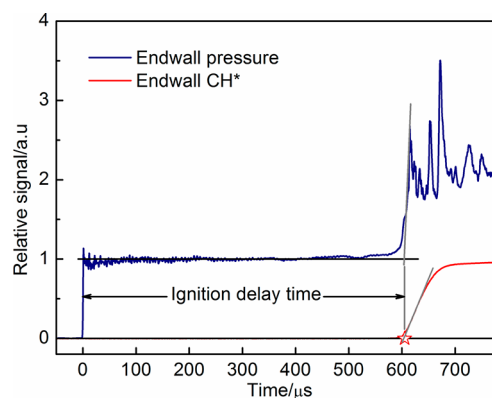

Figure 2. Definition of the ignition delay time.

Table 1. Composition of Fuel Mixtures

mixtures	X_{DME} (%)	$X_{C_4H_{10}}$ (%)	X_{O_2} (%)	X_{Ar} (%)	ϕ
DME100	2.04	0.00	6.12	91.84	1.0
DME70	1.06	0.46	6.16	92.32	1.0
DME30	0.34	0.79	6.18	92.69	1.0
DME00	0.00	0.95	6.19	92.86	1.0

diluent gas because its lack a vibrational mode, which eliminates consideration of the time scale for vibrational relaxation when calculating the post-shock conditions. Additionally, reflected shock pressure profiles for argon mixtures usually display less noise because of the lack of (or smaller) sidewall bifurcation relative to nitrogen. Hence, optimized reflected shock conditions are typically obtained using dilute mixtures in argon. The DME blending ratio is defined as $\phi_{DME} = X_{DME}/(X_{DME} + X_{n\text{-butane}})$, where X_{DME} and $X_{n\text{-butane}}$ are the mole fractions of DME and n-butane. ϕ_{DME} values of 0, 30, 70, and 100% are chosen for the study. Post-reflected shock pressures (p) are selected as 1.2 and 5.3 atm. Ignition temperatures (T) are calculated with Gaseq.[22] Purities of oxygen, argon, DME, and n-butane are 99.995, 99.995, 99.9, and 99.9%, respectively. Table 2 gives the measured ignition delay times of DME/n-butane mixtures in this study.

Calculations were made using the Senkin[23] code in the Chemkin II package[24] with the constant volume adiabatic model. The computed ignition delay time is defined as the time interval between zero and the maximum rate of temperature rise (max dT/dt) in the study. The chemical kinetic model used in the study is the NUI C4_47 mechanism developed by Curran et al.[25] It includes the oxidation mechanism of C_1–C_4 HCs and a DME submodel. The NUI C4_47 mechanism consists of 226 species and 1319 elementary reactions.

3. RESULTS AND DISCUSSION

3.1. Ignition Delay Time Measurements. Figure 3 gives the measured ignition delay times of DME/n-butane blends at different pressures. Results show that ignition delay times at various test conditions show a good linear dependence upon $1000/T$. Therefore, fitted correlations of ignition delay times as a function of p and T for each fuel mixture are obtained through regression as follows:

$$\tau = 3.31 \times 10^{-4} p^{-0.47} \exp\left(\frac{39.1 \pm 0.9 \text{ kcal mol}^{-1}}{R_u T}\right),$$
$$R^2 = 0.994 \tag{1}$$

for DME00, with p = 1.2−5.3 atm and T = 1250−1510 K

$$\tau = 5.56 \times 10^{-4} p^{-0.50} \exp\left(\frac{37.4 \pm 0.9 \text{ kcal mol}^{-1}}{R_u T}\right),$$
$$R^2 = 0.990 \tag{2}$$

for DME30, with p = 1.2−5.3 atm and T = 1240−1500 K

$$\tau = 4.80 \times 10^{-4} p^{-0.53} \exp\left(\frac{37.3 \pm 0.6 \text{ kcal mol}^{-1}}{R_u T}\right),$$
$$R^2 = 0.996 \tag{3}$$

for DME70, with p = 1.2−5.3 atm and T = 1170−1500 K

$$\tau = 2.45 \times 10^{-4} p^{-0.57} \exp\left(\frac{38.7 \pm 0.6 \text{ kcal mol}^{-1}}{R_u T}\right),$$
$$R^2 = 0.997 \tag{4}$$

for DME100, with p = 1.2−5.3 atm and T = 1200−1650 K, where τ is the ignition delay time in μs, p is the pressure in atm, R_u = 1.986 × 10^{-3} kcal mol^{-1} K^{-1} is the universal gas constant, and T is the temperature in K. The four formulas above have good regressions ($R^2 > 0.99$) to the measured ignition delay times. Because of the limited range of the study, eqs 1−4 correlations are suitable to the limited pressure and temperature range for the stoichiometric mixtures.

For each mixture, ignition delay times are decreased with an increase in the pressure. This indicates that high pressure can promote the ignition, which corresponds to the negative pressure exponent in eqs 1−4. With the increase of the DME blending ratio, the absolute value of the pressure exponent is increased and the effect of the pressure on the ignition delay time is increased.

3.2. Ignition Delay Time Calculations. Figure 4 gives the comparison between the measured and calculated ignition delay times of DME/n-butane blends. When the temperature is higher than 1400 K, the numerical predictions agree well with experimental data for the four mixtures at pressures of 1.2 and 5.3 atm. When the temperature is lower than 1400 K, the numerical predictions give an overprediction to the experimental data.

Table 2. Measured Ignition Delay Times of DME/n-Butane Mixtures

|	DME00			DME30			DME70			DME100	
p (atm)	T (K)	τ (μs)	p (atm)	T (K)	τ (μs)	p (atm)	T (K)	τ (μs)	p (atm)	T (K)	τ (μs)
1.25	1253	1791	1.22	1238	1849	1.23	1299	791	1.20	1436	155
1.39	1332	797	1.21	1297	902	1.24	1372	388	1.33	1375	300
1.49	1386	485	1.23	1376	438	1.14	1353	460	1.29	1316	610
1.24	1450	267	1.26	1458	226	1.23	1430	222	1.29	1236	1336
1.23	1511	155	1.23	1511	142	1.25	1506	110	1.27	1527	74
1.24	1585	70	1.21	1541	92	1.21	1534	88	1.28	1591	50
1.24	1250	1898	1.24	1611	62	1.24	1234	1664	1.29	1670	29
1.23	1276	1432	1.21	1391	369	5.42	1265	614	5.49	1343	199
5.46	1281	814	5.38	1346	321	5.45	1336	256	5.34	1271	472
5.50	1355	322	5.16	1379	175	5.25	1173	1884	5.33	1192	1293
5.30	1400	199	5.41	1488	68	5.45	1459	70	5.30	1405	107
5.32	1477	93	5.37	1273	746	5.44	1402	143	4.95	1478	49
5.42	1543	46	5.36	1220	1192	5.26	1275	451	5.22	1568	22
5.44	1230	1457	5.49	1326	389	5.32	1216	960	5.26	1652	12
			5.44	1457	95	5.54	1451	85			
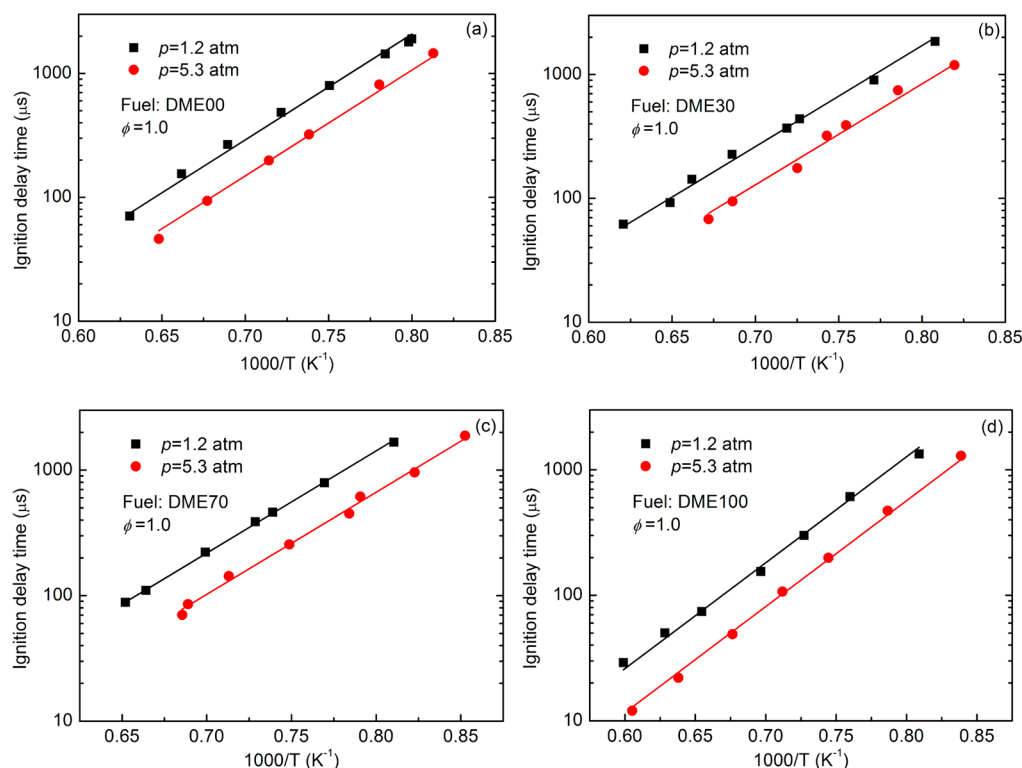
Figure 3. Measured ignition delay times of DME/*n*-butane blends at different pressures (symbols, measured values; lines, fitted values using eqs 1−4): (a) DME00, (b) DME30, (c) DME70, and (d) DME100.
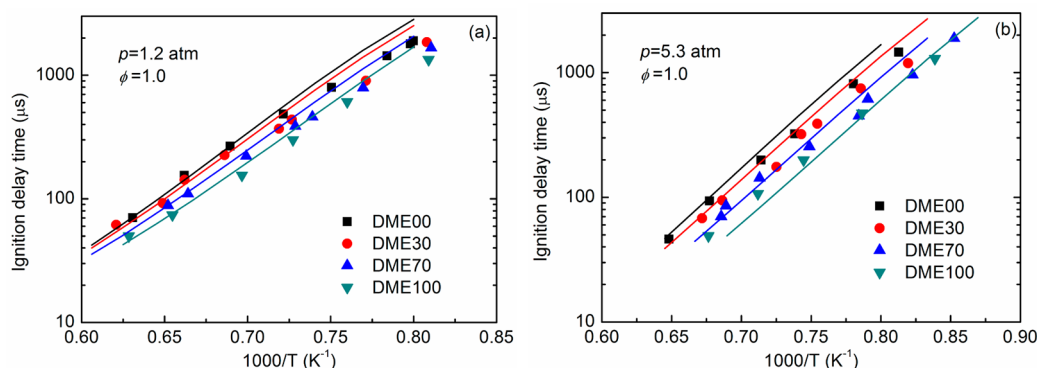

Figure 4. Measured and calculated ignition delay times of DME/*n*-butane blends (symbols, measured values; lines, calculated values): (a) $p = 1.2$ atm and (b) $p = 5.3$ atm.

On the basis of the consideration of the applicable conditions of eqs 1−4 and the calculated results in Figure 4, the temperature of 1500 K is chosen for the chemical kinetic analysis in the following text. Figure 5 shows the calculated and fitted ignition delay times using eqs 1−4 for the DME/*n*-butane blends at different DME blending ratios at the temperature of 1500 K. Ignition delay times decrease with an increasing DME blending ratio, and the calculations are reasonably consistent with the fitted results at all DME blending ratios.

H and OH are the important radicals for the ignition chemical reactions. Almost all chain reactions are related to them, and their concentrations play an important role in the ignition of DME/*n*-butane blends. Figure 6 gives the H and OH profiles at different DME blending ratios, at $p = 1.2$ atm and $T = 1500$ K. On the one hand, the timing at rapid increase in H and OH mole fractions advances with an increasing DME blending ratio (for example, 0.16 ms for the *n*-butane mixture

and 0.10 ms for the DME mixture). On the other hand, the peak values of the H and OH mole fractions also increase with an increasing DME blending ratio. These H and OH enhancements promote the ignition of DME/*n*-butane blends with an increasing DME blending ratio.

3.3. Analysis on the Reaction Pathway. Figures 7 and 8 give the reaction pathway for the stoichiometric DME and *n*-butane mixtures at $p = 1.2$ atm and $T = 1500$ K, respectively. The timing at which 20% fuel consumed was selected by Black et al.[26] and Weber et al.[27] Reaction pathways of DME consumption for the DME100 and DME70 mixtures are almost the same, and reaction pathways of *n*-butane consumption for the DME00 and DME30 mixtures are also almost the same. This indicates that, for a specified fuel, the reaction pathways of its consumption are the same whether it is a pure fuel or the fuel blend.
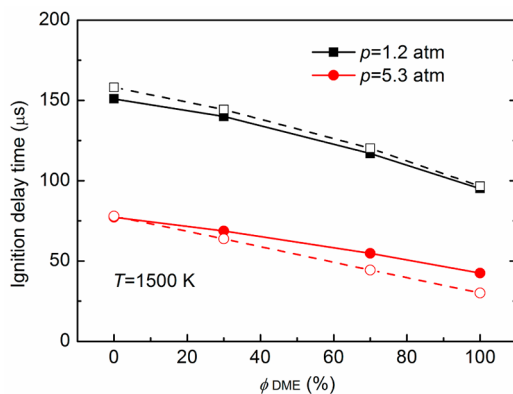
Figure 5. Fitted and calculated ignition delay times of DME/*n*-butane blends at varied DME blending ratios (solid lines, fitted results from eqs 1−4; dash lines, calculated results).

Figure 7. Reaction pathway of DME in a shock tube at p = 1.2 atm, T = 1500 K, and ϕ = 1.0 (bold font, DME100; normal font, DME70).

Figure 8. Reaction pathway of *n*-butane in a shock tube at p = 1.2 atm, T = 1500 K, and ϕ = 1.0 (bold font, DME00; normal font, DME30).

For the DME100 mixture, 30% of CH_3OCH_3 is consumed through the unimolecular decomposition reaction R353, which produces CH_3O and CH_3 radicals. A total of 70% of CH_3OCH_3 is consumed through hydrogen-abstraction reactions by OH, H, O, and CH_3 (R354, R355, R356, and R359), which produces CH_3OCH_2 radicals. A total of 82% of CH_3O decays into CH_2O and H atoms via hydrogen abstraction following β-scission through R63, and the other 18% of CH_3O is consumed through hydrogen-abstraction reactions by O_2 and CH_3 (R64 and R67).[28] CH_3OCH_2 decomposes to CH_2O and CH_3 through β-scission.

For the DME00 mixture, 35% of C_4H_{10} decomposes to CH_3, C_2H_5, and NC_3H_7 radicals by breaking C−C bonds through unimolecular decomposition reactions (R668 and R669). Because of two different H positions in the C_4H_{10} molecule, 41% of C_4H_{10} and 22% of C_4H_{10} are consumed by hydrogen-abstraction reactions and generate SC_4H_9 and PC_4H_9, respectively. A total of 85% of C_2H_5 generates C_2H_4 by hydrogen-abstraction reactions. NC_3H_7 is consumed by β-scission reactions (R455 and R456) to produce C_2H_4 and C_3H_6. SC_4H_9 and PC_4H_9 are consumed by β-scission reactions (R716 and R715) and generate C_3H_6 and C_2H_5, respectively.

3.4. Sensitivity Analysis. Sensitivity analysis on the dependence of the ignition delay time upon the DME blending ratio is performed, as shown in Figure 9. The normalized sensitivity is defined as $S = [\tau(2.0k_i) - \tau(0.5k_i)]/1.5\tau(k_i)$, where τ is the ignition delay time and k_i is pre-exponential factor of the *i*th reaction. A negative value of S indicates the promotion influence on the overall reaction rate and vice versa.
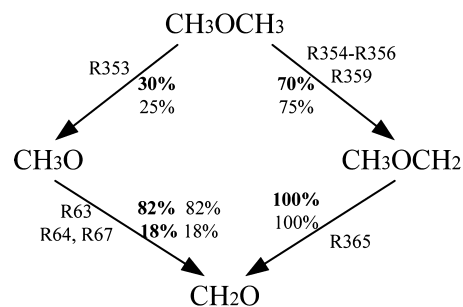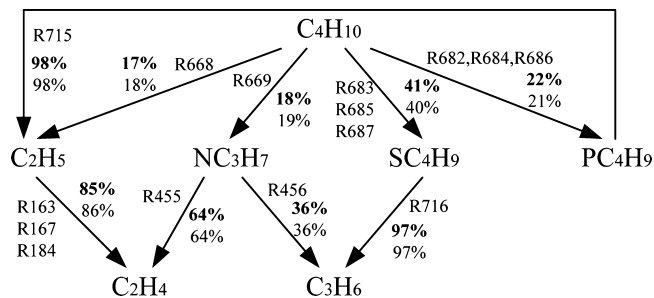
Reaction R1 gives the highest sensitive coefficient, which indicates that R1 dominates the ignition process of the DME/*n*-butane mixture. Among these 12 element reactions with a high sensitivity factor, there are three reactions (R668, R685, and R683) related to the butane molecule and only one reaction (R355) related to the DME molecule, while the rest are the reactions that involve the participation of small molecules. With the decrease of the DME blending ratio, the sensitivity factor and its variation of R683 show the largest values among all positive sensitivity factors and the sensitivity factor and its variation of R1 give the largest values among all negative sensitivity factors.

Figure 10 gives the reaction rates of R683 and R1 at different DME blending ratios. A decrease in the DME blending ratio increases the sensitivity factor of R683. Meanwhile, the reaction rate of R683 also increases with a decreasing DME blending ratio. This induces the increase of the ignition delay time from the positive sensitivity factor of R683. As the DME blending ratio is decreased, the absolute value of the sensitivity factor of R1 increases and the reaction rate decreases. This also increases
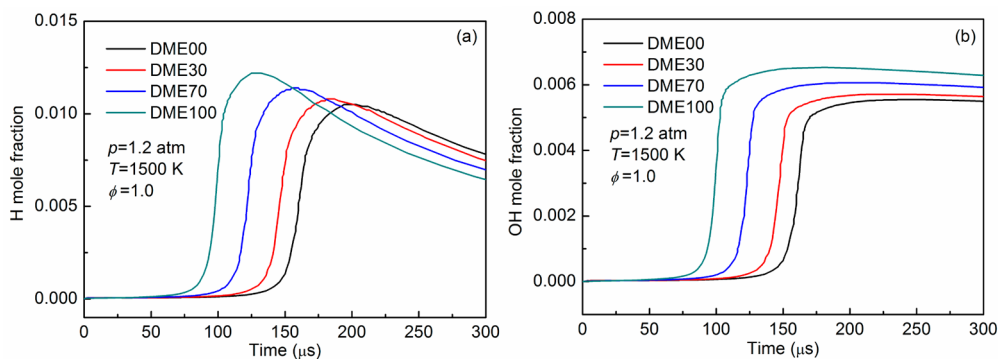

Figure 6. H and OH profiles at varied DME blending ratios: (a) H radical and (b) OH radical.
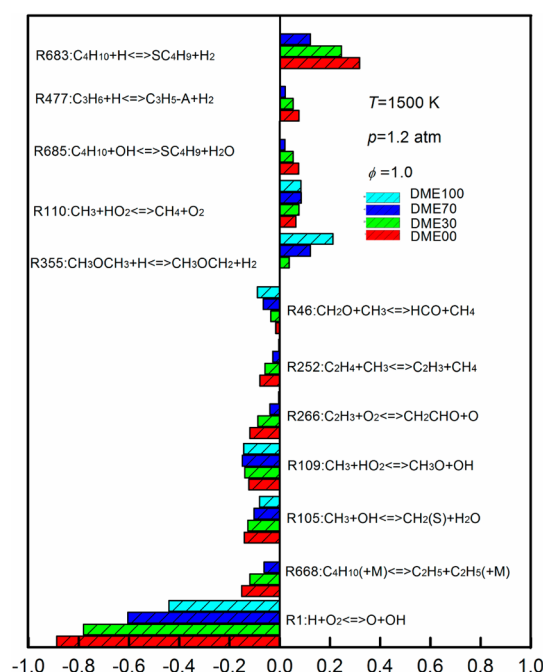
Figure 9. Sensitive analysis of the ignition delay time at varied DME blending ratios.

the ignition delay time from the negative sensitivity factor of R1.

4. CONCLUSION

Experimental and kinetic studies on ignition delay times of DME/n-butane/O_2/Ar mixtures with varied DME blending ratios were conducted using the shock tube and Chemkin package. The main conclusions are as follows: (1) Correlations of ignition delay times as a function of p and T are obtained through regression analysis of the measured data. An increase in the pressure and DME blending ratio promotes the ignition. With an increasing DME blending ratio, the absolute value of the pressure exponent increases and the effect of pressure on the ignition delay time is promoted. (2) Numerical predictions agree well with experimental data for the four fuel mixtures at temperatures higher than 1400 K. At temperatures lower than 1400 K, the numerical predictions give an overprediction of the experimental data. The peak values of H and OH mole fractions increase with an increasing DME blending ratio, and

they promote the ignition of DME/n-butane blends. (3) The reaction pathway shows that hydrogen-abstraction reactions play the dominant role in the consumption of fuel rather than the unimolecular decomposition reactions. Chemical reactions of two fuel components are independent.

■ ASSOCIATED CONTENT

ⓢ Supporting Information

Dominant elementary reactions in this study. This material is available free of charge via the Internet at http://pubs.acs.org.

■ AUTHOR INFORMATION

Corresponding Author

*Telephone: 86-29-82665075. Fax: 86-29-82668789. E-mail: zhhuang@mail.xjtu.edu.cn.

Notes

The authors declare no competing financial interest.

■ ACKNOWLEDGMENTS

■ REFERENCES

(1) Westbrook, C. K.; Warnatz, J.; Pitz, W. J. A detailed chemical kinetic reaction mechanism for the oxidation of *iso*-octane and *n*-heptane over an extended temperature range and its application to analysis of engine knock. *Proc. Combust. Inst.* **1989**, *22* (1), 893−901.

(2) Sato, S.; Jun, D.; Kweon, S.; Yamashita, D.; Iida, N. Basic research on the suitable fuel for HCCI engine from the viewpoint of chemical reaction. *SAE [Tech. Pap.]* **2005**, DOI: 10.4271/2005-01-0149.

(3) Kong, S. A study of natural gas/DME combustion in HCCI engines using CFD with detailed chemical kinetics. *Fuel* **2007**, *86* (10−11), 1483−1489.

(4) Lee, S.; Oh, S.; Choi, Y. Performance and emission characteristics of an SI engine operated with DME blended LPG fuel. *Fuel* **2009**, *88* (6), 1009−1015.

(5) Iida, N.; Yoon, H. Combustion research on internal combustion engine focus on homogeneous charge compression ignition. *SAE [Tech. Pap.]* **2009**, DOI: 10.4271/2009-32-0189.

(6) Ozaki, J.; Iida, N. Effect of degree of unmixedness on HCCI combustion based on experiment and numerical analysis. *SAE [Tech. Pap.]* **2006**, DOI: 10.4271/2006-32-0046.
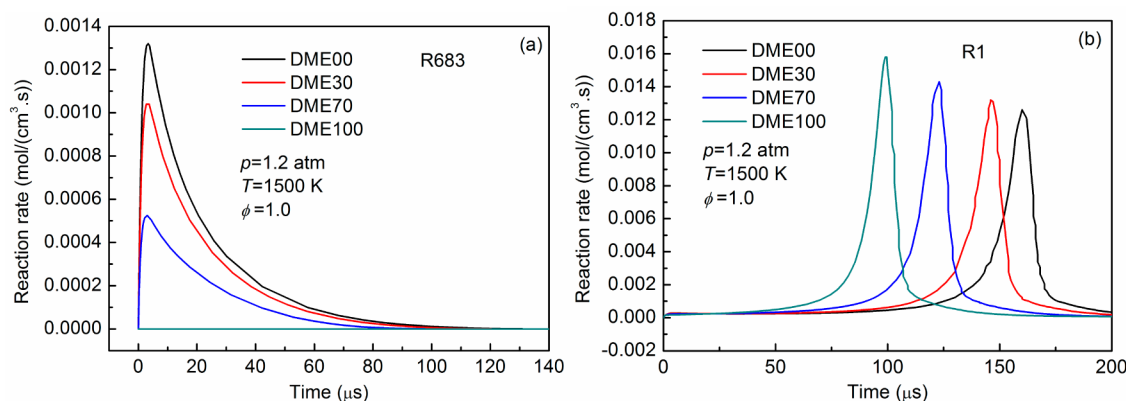
Figure 10. Reaction rates of R683 and R1 at varied DME blending ratios: (a) R683 and (b) R1.

(7) Liang, C.; Ji, C. W.; Gao, B. B.; Liu, X. L.; Zhu, Y. M. Investigation on the performance of a spark-ignited ethanol engine with DME enrichment. *Energy Convers. Manage.* **2012**, *58*, 19−25.

(8) Ji, C. W.; Liang, C.; Wang, S. F. Investigation on combustion and emissions of DME/gasoline mixtures in a spark-ignition engine. *Fuel* **2011**, *90* (3), 1133−1138.

(9) Liang, C.; Ji, C. W.; Gao, B. B.; Liu, X. L. Combustion and emissions performance of a DME-enriched spark-ignited methanol engine at idle condition. *Appl. Energy* **2011**, *88* (11), 3704−3711.

(10) Ji, C. W.; Liang, C.; Zhu, Y. M.; Liu, X. L.; Gao, B. B. Investigation on idle performance of a spark-ignited ethanol engine with dimethyl ether addition. *Fuel Process. Technol.* **2012**, *94* (1), 94−100.

(11) Lu, X. C.; Han, D.; Huang, Z. Fuel design and management for the control of advanced compression-ignition combustion modes. *Prog. Energy Combust.* **2011**, *37* (6), 741−783.

(12) Huang, C.; Yao, M. F.; Lu, X. C.; Huang, Z. Study of dimethyl ether homogeneous charge compression ignition combustion process using a multi-dimensional computational fluid dynamics model. *Int. J. Therm. Sci.* **2009**, *48* (9), 1814−1822.

(13) Pfahl, U.; Fieweger, K.; Adomeit, G. Self-ignition of diesel-relevant hydrocarbon−air mixtures under engine conditions. *Proc. Combust. Inst.* **1996**, *26* (1), 781−789.

(14) Mittal, G.; Chaos, M.; Sung, C. J.; Dryer, F. L. Dimethyl ether autoignition in a rapid compression machine: Experiments and chemical kinetic modeling. *Fuel Process. Technol.* **2008**, *89* (12), 1244−1254.

(15) Dagaut, P.; Daly, C.; Simmie, J. M.; Cathonnet, M. The oxidation and ignition of dimethylether from low to high temperature (500−1600 K): Experiments and kinetic modeling. *Proc. Combust. Inst.* **1998**, *27*, 361−369.

(16) Cook, R. D.; Davidson, D. F.; Hanson, R. K. Shock tube measurements of ignition delay times and OH time histories in dimethyl ether oxidation. *Proc. Combust. Inst.* **2009**, *32*, 189−196.

(17) Zhao, Z.; Chaos, M.; Kazakov, A.; Dryer, F. L. Thermal decomposition reaction and a comprehensive kinetic model of dimethyl ether. *Int. J. Chem. Kinet.* **2008**, *40* (1), 1−18.

(18) Amano, T.; Dryer, F. L. Effect of dimethyl ether, NO_x, and ethane on CH_4 oxidation: High pressure, intermediate-temperature experiments and modeling. *Proc. Combust. Inst.* **1998**, *27* (1), 397−404.

(19) Chen, Z.; Qin, X.; Ju, Y. G.; Zhao, Z. W.; Chaos, M.; Dryer, F. L. High temperature ignition and combustion enhancement by dimethyl ether addition to methane−air mixtures. *Proc. Combust. Inst.* **2007**, *31*, 1215−1222.

(20) Zhang, Y. J.; Huang, Z. H.; Wei, L. J.; Zhang, J. X.; Law, C. K. Experimental and modeling study on ignition delays of lean mixtures of methane hydrogen oxygen argon at elevated pressures. *Combust. Flame* **2012**, *159* (3), 918−931.

(21) Zhang, J. X.; Wei, L. J.; Man, X. J.; Jiang, X.; Zhang, Y. J.; Hu, E. J.; Huang, Z. H. Experimental and modeling study of *n*-butanol oxidation at high temperature. *Energy Fuels* **2012**, *26*, 3368−3380.

(22) Morley, C. *Gaseq, Version 0.76*; http://www.gaseq.co.uk.

(23) Lutz, A. E.; Kee, R. J.; Miller, J. A. *SENKIN: A Fortran Program for Predicting Homogeneous Gas Phase Chemical Kinetics with Sensitivity Analysis*; Sandia National Laboratories: Albuquerque, NM, 1988; SAND87-8248.

(24) Kee, R. J.; Rupley, F. M.; Miller, J. A. *CHEMKIN-II: A Fortran Chemical Kinetics Package for the Analysis of Gas-Phase Chemical Kinetics*; Sandia National Laboratories: Albuquerque, NM, 1989; SAND89-8009.

(25) Donato, N.; Aul, C.; Petersen, E.; Zinner, C.; Curran, H. J.; Bourque, G. Ignition and oxidation of 50/50 butane isomer blends. *J. Eng. Gas Turbines Power* **2010**, *132* (5), No. 051502.

(26) Black, G.; Curran, H. J.; Pichon, S.; Simmie, J. M.; Zhukov, V. Bio-butanol: Combustion properties and detailed chemical kinetic model. *Combust. Flame* **2010**, *157* (2), 363−373.

(27) Weber, B.; Kumar, K.; Sung, C. J. Autoignition of butanol isomers at low to intermediate temperature and elevated pressure. *Proceedings of the 49th American Institute of Aeronautics and Astronautics (AIAA) Aerospace Sciences Meeting*; Orlando, FL, Jan 4−7, 2011; Paper AIAA-2011-316.

(28) Turns, S. R. *An Introduction to Combustion: Concepts and Applications*; McGraw-Hill: New York, 2011.